Theory of Inhomogeneous Polymers. Solutions for the Interfaces of the Lattice Model

Thomas A. Weber and Eugene Helfand*

Bell Laboratories, Murray Hill, New Jersey 07974. *Received September 22, 1975*

ABSTRACT: The equations for the lattice model of concentrated polymer solution interfaces are solved numerically to provide surface tensions, concentration profiles, and polymer bond anisotropy factors. Systems studied in pure polymer against a wall, polymer solutions against a wall with or without an adsorption potential, and the interface between a saturated polymer solution and the solvent. Qualitative discussion is presented of how the observed effects relate to polymer anisotropy and solvent adsorption in the interphase. The numerical methods used to solve the equations are outlined.

In the previous paper[1] a theory of interfaces of concentrated polymer solutions was developed employing a lattice model. Here we shall present numerical solutions to the equations, at the same time attempting to relate the deduced behavior to a qualitative description of how entropy and energy control the situation.

There are several specific types of interfaces which we may consider. A great deal of insight is gained by examining the case of a pure polymer which fills a lattice, but is confined by an inpenetrable wall. We will see, in unadorned form, the type of anisotropy induced in a polymer near an interface, and observe how this leads to a loss of conformational entropy. It is then possible to understand the changes which solvent induces in terms of how solvent distribution relieves the conformational entropy loss. We shall also see how the solvent density profile can be shifted by specific adsorptive energies.

The above cases deal with polymeric systems against a wall. In many ways surfaces against vacuum and saturated polymer solutions against solvent behave similarly.

The paper concludes with a section on numerical methods of solution of the coupled set of equations for this lattice model. The techniques used were quite general and may be applied to even more complex models of the interfaces.

I. The Lattice Model and Equations

We begin this work with a rapid guide through paper I.[1] The model was defined in section I of that paper, which should be read entirely.

In section II attention was directed to the probability of various conformations of the polymer and solvent. In particular one considered the probability, $p(\mathbf{r}_k|\mathbf{r}_{k-1};k)$, that a polymer unit labeled k is in cell $\mathbf{r}_k$, given that the previous unit along the chain is in cell $\mathbf{r}_{k-1}$. Under homogeneous conditions the unit k is equally likely to be in any of the z cells neighboring $\mathbf{r}_{k-1}$, so p would be $1/z$. However, let us consider inhomogeneous conditions, where in layer l the volume fractions of the solvent and polymer are $\varphi_{l\mathrm{o}}$ and $\varphi_{l\mathrm{P}}$, respectively. Then the probability must contain an anisotropy factor:

$$p(\mathbf{r}_k|\mathbf{r}_{k-1};k) = g_l^{\nu}/z \tag{I.1}$$

Here l is the layer of $\mathbf{r}_{k-1}$ and $\nu = +, 0, -$ according to whether the bond from unit $k-1$ to k is directed to a higher, the same, or a lower layer (for further detail see the paragraph containing II.4 in paper I). We see that a g_l^{ν} greater than unity indicates a greater than random probability for bonds from level l to be in direction ν.

The entropy of mixing is given by II.19 in paper I. The $\varphi_{l\mathrm{o}} \log \varphi_{l\mathrm{o}}$ term is the appropriate generalization of the Flory–Huggins entropy,[2] and not surprisingly, a sum of g_l^{ν} $\log g_l^{\nu}$ terms arises from the bond anisotropy. The heat of mixing, eq III.1 in paper I, is taken in random mixing form, and contains a term which accounts for specific surface interactions between the wall and material in the first layer. The heat and entropy can be combined to form a free-energy expression, eq III.2 in paper I, and a surface tension, eq III.6 in paper I. Finally, eq IV.7–12 in paper I for the density profile and anisotropy factors are obtained by minimizing the free energy, subject to appropriate constraints, eq IV.1–5 in paper I. The most important constraints to recall here are: full occupancy

$$\varphi_{l\mathrm{P}} + \varphi_{l\mathrm{o}} = 1 \tag{I.2}$$

normalization of g_l^{ν}

$$mg_l^{+} + (1-2m)g_l^{0} + mg_l^{-} = 1 \tag{I.3}$$

and the flux constraint

$$\varphi_{l\mathrm{P}}g_l^{+} = \varphi_{l+1,\mathrm{P}}g_{l+1}^{-} \tag{I.4}$$

which expresses the equality of number of bonds going up from layer l and those coming down from layer $l+1$.

II. Numerical Results and Discussion

In this section we will present the results of solutions of the equations of the lattice model of interfaces. Throughout, our emphasis will be on providing a qualitative description of the observed results. It should be borne in mind that the equations to be solved are derived on the basis of a mean field theory. We shall see that there are many states with free energies not widely differing from the minimum in certain cases. Hence fluctuations may produce quantitative differences in the real systems.

A. Pure Polymer Against a Hard Wall. We will clearly see the effect of polymer bond anisotropy by considering a pure polymer against a hard wall. Immediately we know that $\varphi_{l\mathrm{P}} = 1$, $l \geq 1$. In Table I the anisotropy factors for this system are listed. Inpenetrability of the wall dictates that $g_1^{-} = 0$. The normalization condition, eq I.3, becomes

$$(1-2m)g_1^{0} + mg_1^{+} = 1$$

so we may expect g_1^{0} and g_1^{+} to be greater than unity, but we still must decide the distribution between bonds in the 0 and + directions. Consider two extreme criteria (the truth lies between). In the first we will uncouple the equations by maximizing separately what might be called the entropy of each layer:

$$mg_l^{-} \log g_l^{-} + (1-2m)g_l^{0} \log g_l^{0} + mg_l^{+} \log g_l^{+} \tag{II.1}$$

With $g_1^{-} = 0$, the equation

$$g_1^{0} = g_1^{+} = (1-m)^{-1}$$

maximizes eq II.1 and satisfies the normalization condition

Table I
Polymer Against a Hard Wall

m	l	g_l^-	g_l^0	g_l^+	$F/n_S k_B T$	γ,[a] erg/cm²
1/4	1	0	1.423	1.154	0.2964	4.91
	2	1.154	0.936	0.973		
	3	0.973	1.011	1.004		
	4	1.004	0.998	0.999		
1/6	1	0	1.2262	1.0954	0.1842	3.05
	2	1.0954	0.9786	0.9903		
	3	0.9903	1.0022	1.0010		
	4	1.0010	0.9998	0.9999		

[a] Surface tension figure is based on T = 300 K and a cross-sectional area per cell of 0.25 nm².

eq I.3. (For m = 1/4, $g_1^0 = g_1^+ = 4/3$.) The flux constraint, eq I.4, then dictates that $g_2^- = g_1^+$. Now g_2^- is greater than unity so g_2^0 and g_2^+ may be expected to be less than unity, by normalization. If they are equal the common value is $(1 - 2m)/(1 - m)^2$ (or 8/9 for m = 1/4). What we see is that using the flux constraint and successively maximizing the entropy on each layer leads to $g_l^0 = g_l^+$. This propagates the anisotropy from layer to layer, causing a loss of conformational entropy from succeeding layers. The procedure does not produce, overall, the highest entropy (for m = 1/4 the surface free energy comes out to be $F/n_S k_B T$ = 0.3074, where n_S is the number of cells per layer, k_B is Boltzmann's constant, and T is the temperature). At the other extreme, all propagation of entropy loss to layers beyond l = 1 can be eliminated by selecting $g_1^+ = 1$, after which all g_l^ν ($l \geq 2$) will be unity. Although there is no loss of conformational entropy from layers 2 on, this too does not produce the highest overall entropy ($F/n_S k_B T$ = 0.3041 in this case). The correct solution is a compromise between the two extremes. In Table I we see that g_1^0 and g_1^+ are greater than unity, but they are not equal. Rather, g_1^+ is closer to, but not equal to, unity. Then $g_2^- = g_1^+ > 1$ by the flux constraint, so g_2^+ and g_2^0 are less than unity. Again g_2^+ is closer to unity than g_2^0, etc. This solution corresponds to the minimum free energy ($F/n_S k_B T$ = 0.2964 for m = 1/4).

It will improve our prospective if we convert the entropy loss per unit area of a cell into a surface tension in familiar units. For this purpose we will take as a typical value of the cross sectional area of a cell 0.25 nm² [(Avogadro's No. × 10^3 (kg/m³)/0.1 (kg/unit))$^{-2/3}$] and consider a temperature of 300 K. Then an entropy in units of k_B is converted to a surface tension in erg/cm² by multiplying by 16.566. Thus for m = 1/4 we find 4.91 erg/cm² while for m = 1/6 we have 3.05 erg/cm². (To convert to MKS, 1 erg/cm² = 10^{-3} J/m².)

B. Polymer Solution Against a Hard Wall. What do we expect to happen when solvent is added to the polymer against the wall (and there are no specific wall interactions χ_0 and χ_P)? Polymer suffers a loss of conformational entropy when the bond directions are anisotropic. In the last section we saw that this anisotropy is most severe in the first layer. Hence there is an entropic force moving polymer out of this layer, hence solvent in. Whatever polymer remains in the first layer experiences an anisotropy tending to make g_1^+ greater than unity. The solvent plays a role in decreasing the anisotropy of polymer in layers via the flux constraint, which we write in the form

$$(1 - \varphi_{l0})g_l^+ = (1 - \varphi_{l+1,0})g_{l+1}^- \qquad \text{(II.2)}$$

If g_1^+ is greater than unity we can bring g_2^- closer to unity, helping to attenuate the anisotropy, by making φ_{20} less than φ_{10}. Of course, these two ways of using the solvent concentration to decrease the loss of entropy due to anisotropy must be balanced against the resulting loss of free energy from making the concentration profiles deviate from the bulk value.

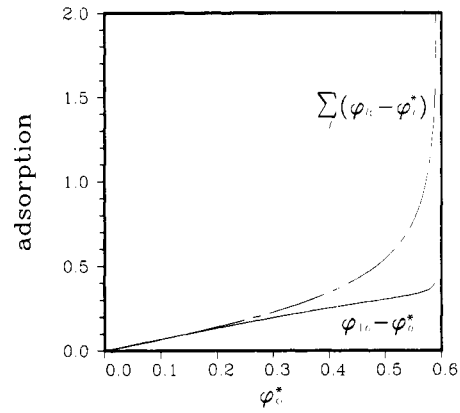

Figure 1. Adsorption of solvent into the first layer ($\varphi_{10} - \varphi_0^*$) and total adsorption of solvent [$\Sigma_l(\varphi_{l0} - \varphi_0^*)$], for a polymer solution against an inpenetrable wall. Adsorption is plotted as a function of the asymptotic solvent concentration, φ_0^*. The solvent is a fairly poor one (χ = 0.7), and m = 1/4. As φ_0^* approaches its saturation value of 0.590 the solvent excess at the wall becomes large.

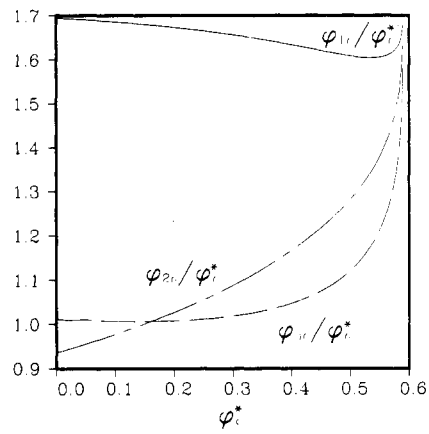

Figure 2. A measure of the adsorption of solvent into the first three layers near the wall for a polymer solution. The tendency toward desorption of solvent from layer 2 arises from a coupling to polymer bond anisotropy as explained in the text (χ = 0.7, m = 1/4).

All of this is illustrated in the explicit numerical results. We study the case of a lattice with m = 1/4 and a solvent of fairly poor quality, χ = 0.7. In Figure 1 we see that solvent is adsorbed to the surface region, indeed in larger amounts as the bulk concentration of solvent increases. Most of this adsorption is into the first layer, except for concentrations of solvent in the solution, φ_0^*, approaching saturation (φ_0^* = 0.5897). Near saturation a bulk phase of solvent is getting to be almost stable thermodynamically. Thus the free-energy gain of keeping polymer from the wall largely offsets the free-energy loss of creating many solvent-rich layers.

Away from near-saturation concentrations of solvent, we see manifestations of the way that the solvent concentration profile can be used to attenuate polymer anisotropy, as discussed above. In Figure 2 we note that in some cases this can lead to a net desorption of solvent from layer 2. We see in Figure 3 that for low φ_0^* the adjustment of solvent concentration in the various layers has brought about a decrease in the effects of polymer anisotropy. The ratio of the anisotropy factors in the first layer, g_1^0/g_1^+, is brought toward unity to maximize the randomness of orientation in layer 1. Also g_2^+ is kept near 1 to minimize the propagation of anisotropy to further layers. As the bulk concentration of polymer increases the amount of solvent in the first layer

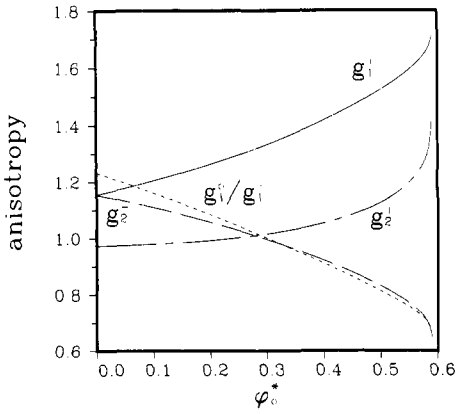

Figure 3. Measures of the polymer bond directional anisotropies for a polymer solution near a wall ($\chi = 0.7$, $m = 1/4$).

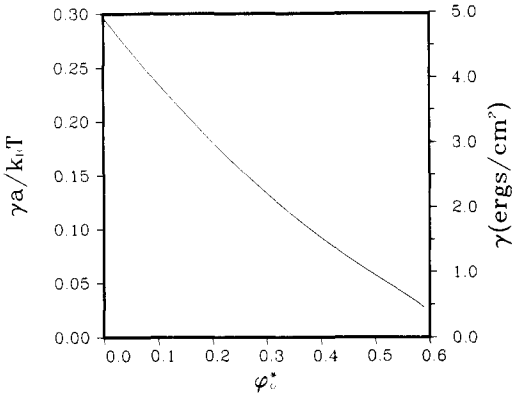

Figure 4. Surface tension vs. the asymptotic polymer solution concentration, φ_0^*. The solvent parameters are $\chi = 0.7$ and $m = 1/4$. The left-hand scale is in reduced units, while the right-hand scale assumes typical parameter values $T = 300$ K and cell cross-sectional area $a = 25$ Å^2.

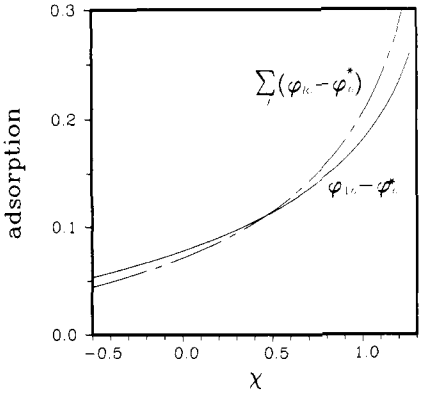

Figure 5. Adsorption as a function of solvent quality. High χ corresponds to low solvation power. Adsorption, as measured by adsorption of solvent into the first layer and by the solvent excess, is more favorable for a poor solvent. The asymptotic solvent concentration, φ_0^*, is fixed at 0.2, which corresponds to a maximum χ value of 1.265 ($m = 1/4$).

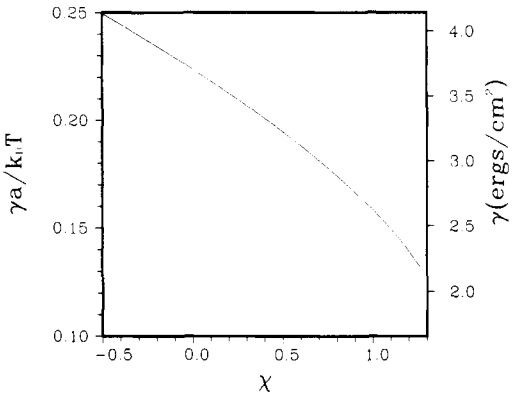

Figure 6. The surface tension decreases with decreasing solvent quality, as shown in the plot of surface tension vs. χ ($\varphi_0^* = 0.2$, $m = 1/4$).

increases more rapidly, so that the anisotropy of the remaining polymer in that layer is of lesser import. The major consideration becomes one of getting polymer which may be in layer 1 out of that layer, which requires that g_1^+ grow. On the other hand, g_2^- decreases so as to avoid sending polymer into layer 1.

In Figure 4 we see that the total surface tension decreases as the concentration of solvent in the solution increases.

Another way to look at the data is to see how quality of the solvent effects surface properties for a given polymer solution of fixed solution concentration. In Figures 5 and 6 we take the solvent concentration as 0.2, and vary χ between −0.5, an excellent solvent with exothermic mixing, and 1.265, at which point the solution is saturated. The better the solvent quality, the less tendency the system has for adsorption of solvent to the surface, as seen in Figure 5. The result is that polymer anisotropy effects cannot be relieved, and any concentration inhomogeneity is expensive in free energy, so that the high quality solvents manifest larger surface tension.

C. Polymer Solution Against a Wall with Adsorption Potential. Let us consider a wall which preferentially adsorbs solvent or polymer units via the potential term in eq III.1 in paper I involving χ_o and χ_P. We will take as a reference state pure solvent against the wall, hence $\chi_o = 0$ and

$$\Delta\chi_W = \chi_P - \chi_o \qquad \text{(II.3)}$$

will be just χ_P. To convert the resulting surface tensions back to absolute units we must add $m\chi_o n_S k_B T$ to the calculated γA (which we will not do here).

The preferential adsorption (or desorption) of solvent (polymer) to the wall, as induced by a positive (negative) $\Delta\chi_W$, leads to a complex interplay among the first layer concentrations, succeeding layer concentrations, and polymer anisotropy. A manifestation of this we show in Figure 7 which depicts surface layer and total absorption vs. adsorption potential $\Delta\chi_W$ for a system with $\chi = 0.7$, $\varphi_0^* = 0.2$, and $m = 1/4$. For contrast we indicate what adsorption to the first layer looks like if we naively assume a simple Boltzman factor enhancement of solvent concentration:

$$\frac{\varphi_{1o}{}^m}{\varphi_{1P}{}^m} = \frac{\varphi_{1o}(\Delta\chi_W = 0)}{\varphi_{1P}(\Delta\chi_W = 0)} \exp(m\Delta\chi_W) \qquad \text{(II.4)}$$

We see that this seriously underestimates the amount of solvent drawn to the surface layer.

Figure 8 shows the surface tension as a function of $\Delta\chi_W$ for this system. The part of the surface tension other than that due to interaction energy with the wall

$$\gamma - m\varphi_{1P}\Delta\chi_W \qquad \text{(II.5)}$$

is also depicted.

D. Polymer Solution–Solvent Interface. We will next consider the interface between a saturated polymer solution and the solvent. Since we are assuming very high molecular weight for the polymer the solvent phase is pure. According to the Flory–Huggins theory the solvent–poly-

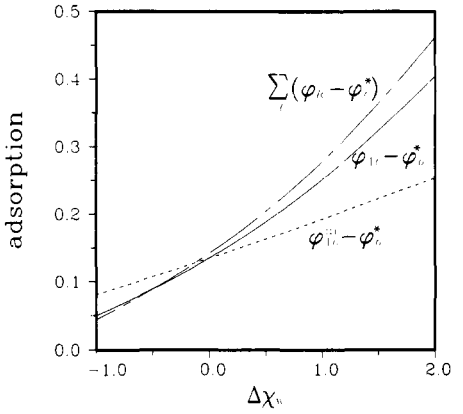

Figure 7. Excess solvent in the first layer, and total excess solvent, increases with an attractive (positive) wall potential $\Delta\chi_W$ and decreases with a repulsive (negative) wall potential $\Delta\chi_W$. The dashed curve, a simple Boltzmann factor estimate of the wall effect (see eq II.4), is seen to be a serious underestimation of the effect. System parameters are $\chi = 0.7$, $\varphi_o^* = 0.2$, and $m = 1/4$.

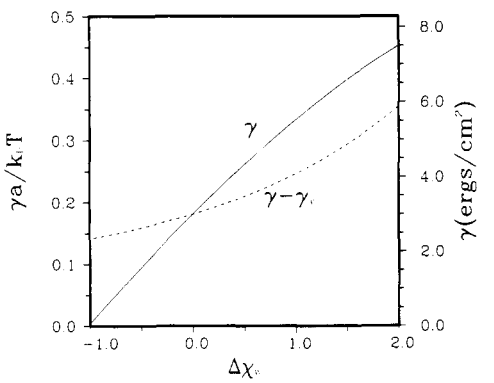

Figure 8. Surface tension of a polymer solution against a wall as a function of wall potential. The solvent adsorption potential, χ_o, is assumed to be zero, $\chi = 0.7$, $\varphi_o^* = 0.2$, and $m = 1/4$. The dashed curve represents the surface tension in excess of the energy of the wall interactions. This surface energy directly due to the wall potential, γ_W, is given by $\gamma_W = \varphi_{1P}\Delta\chi_W k_B T m/a$.

Table II
Saturation Density of Solvent in Polymer Solutions vs. χ

χ	φ_o^*	χ	φ_o^*
5	0.0025	0.8	0.4711
2	0.0699	0.7	0.5897
1.4	0.1617	0.6	0.7557
1.2	0.2225	0.55	0.8653
1.0	0.3162	0.5	1

mer interaction parameter χ must be greater than 1/2, or the solvent will be miscible with the polymer in all proportions. The bulk concentration of solvent in the polymer solution phase is found by equating the chemical potential of the solvent in the two phases, which leads to the equation

$$0 = \chi(1 - \varphi_o^*)^2 + \log \varphi_o^* + (1 - \varphi_o^*) \qquad \text{(II.6)}$$

The solution for φ_o^* as a function of χ is tabulated in Table II.

A sample density profile is illustrated in Figure 9, where φ_{lo} is shown for the various layers l for $\chi = 0.7$ and $m = 1/4$. In the figure also is a plot of the density profile for the Gaussian random-walk model of the polymer, as given by Helfand and Sapse,[3] and adapted to the parameter of the lattice model:

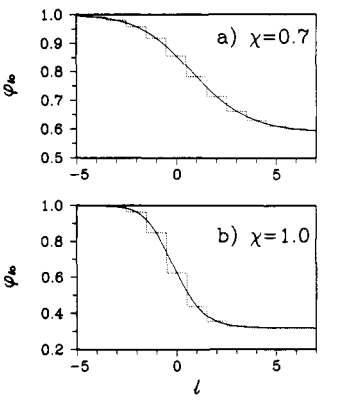

Figure 9. Concentration profile vs. lattice layer for solvent–polymer solution interfaces. The dashed lines are the lattice profiles for $\chi = 0.7$ and 1.0 ($m = 1/4$). The solid curves are the continuous profiles of Helfand and Sapse[3] with the solvent concentration for $l = 0$ set equal to the concentration of the lattice profile at level 0, φ_{0o}.

Table III
Density Profiles and Anisotropies for Solvent–Polymer Solution Interfaces

χ	l	φ_{lo}	g_l^-	g_l^0	g_l^+
2.0	−2	0.9967	0.0413	0.3884	3.182
	−1	0.8889	0.0937	0.7679	2.371
	0	0.3117	0.3827	1.181	1.254
	1	0.0951	0.9541	1.013	1.020
	2	0.0722	0.9948	1.002	1.002
	3	0.0701	0.9997	1.000	1.000
1.5	−3	0.9996	0.1060	0.5477	2.799
	−2	0.9897	0.1184	0.6053	2.671
	−1	0.8633	0.2010	0.8871	2.025
	0	0.4340	0.4892	1.117	1.278
	1	0.1953	0.8986	1.028	1.045
	2	0.1476	0.9868	1.003	1.006
	3	0.1403	0.9978	1.001	1.001
1.0	−4	0.9991	0.3139	0.8080	2.070
	−3	0.9940	0.3201	0.8201	2.040
	−2	0.9650	0.3500	0.8703	1.909
	−1	0.8501	0.4453	0.9770	1.601
	0	0.6240	0.6383	1.046	1.270
	1	0.4369	0.8480	1.030	1.092
	2	0.3544	0.9526	1.010	1.027
	3	0.3275	0.9861	1.003	1.008
	4	0.3194	0.9960	1.001	1.002

$$l = \int^{\varphi_{lo}} d\varphi \left[\frac{m}{4(1-\varphi)} + m\chi\right]^{1/2} \left[\varphi \log \frac{\varphi}{\varphi_o^*} - (\varphi - \varphi_o^*) - \chi(\varphi - \varphi_o^*)^2\right]^{-1/2} \qquad \text{(II.7)}$$

Here l is to be regarded as a continuous variable. The zero of l will be chosen so as to make φ_{0o} agree with the lattice theory. The agreement is not too surprising since the interface is rather broad, so a continuum model of the polymer molecule is reasonable. In Figure 9, however, we also see that for the narrow interface which occurs when $\chi = 1.0$ the Gaussian-model formula fits the profile very well. The $\chi = 1.0$ profile is about the worst fit we get. For larger χ the solvent concentrations jump more rapidly from $\varphi_{lo} = 1$ to φ_o^*. Since one point is fitted, the remaining points do not sensitively test the theory. Density profiles for other values of χ are presented in Table III.

The surface tension of the interface for the lattice model is given by eq III.6 paper I (omitting the final term, the wall potential). A formula for the surface tension of the Gaussian random-walk model is

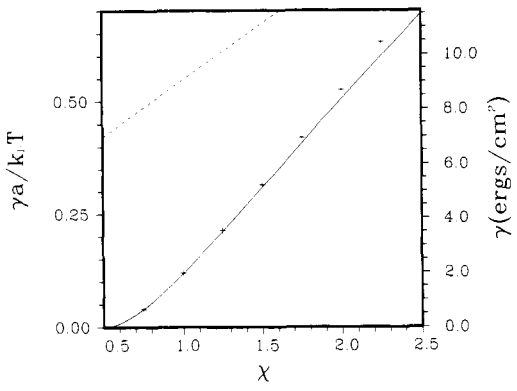

Figure 10. Surface tension vs. solvent quality. Comparison of the surface tension for the lattice model (solid curve) with that of the continuous random walk model (+) is presented. The dashed curve represents asymptotic limit of the surface tension of the lattice model, viz., pure polymer against pure solvent. The right-hand γ scale has T = 300 K and a = 25 Å^2.

$$\frac{\gamma A}{k_B T n_S} = 2\int_{\varphi_o}^{1} d\varphi \left[\frac{m}{4(1-\varphi)} + m\chi\right]^{1/2} \times \left[\varphi \log\frac{\varphi}{\varphi_o^*} - (\varphi - \varphi_o^*) - \chi(\varphi - \varphi_o^*)^2\right]^{1/2} \quad \text{(II.8)}$$

where A is the surface area, so $a \equiv A/n_S$ is the cross-sectional area per cell. The results for both theories are plotted in Figure 10, and agreement is seen to be quite close out to fairly high χ.

For very large χ there must be an abrupt change from polymer to solvent at the interface. An energy of $m\chi k_B T$ arises from interaction across this boundary. Furthermore, the polymer is essentially against an impenetrable barrier. Therefore, the surface tension asymptotically approaches

$$\frac{\gamma a}{k_B T} \sim m\chi + \frac{\gamma_{PW} a}{k_B T} \quad \text{(II.9)}$$

where γ_{PW} is the surface tension (due to conformational entropy loss) of polymer against a hard wall, as reported in Table I. This limit is indicated on Figure 10, but is not closely approached even for $\chi \approx 2$.

III. Numerical Methods of Solution

The methods used to achieve numerical solutions are inspired by techniques developed by Lane[4] for small molecules. A detailed exposition of the polymer solution–solvent interface will be presented. The systems with a wall present are actually simpler and are handled in a similar manner.

The system of equations, eq IV.7–12 in paper I, arising from constrained minimization of the free energy, constitute a triad of difference equations in the sets of variables $\{\xi_l\}$, $\{\lambda_l\}$, and $\{\varphi_{lo}\}$. The variables $\{\lambda_l\}$ may be eliminated to obtain

$$-\xi_l + 2\chi(\varphi_{lo} - \varphi_o^*) + 2m\chi(\varphi_{l+1,o} - 2\varphi_{lo} + \varphi_{l-1,o}) + \log(\varphi_o^*/\varphi_{lo}) = 0 \quad \text{(III.1)}$$

$$\left(2 - \frac{1}{m}\right)\exp(-\xi_l) - \left(\frac{1-\varphi_{l-1,o}}{1-\varphi_{lo}}\right)^{1/2}\exp\left(-\frac{\xi_l + \xi_{l-1}}{2}\right) - \left(\frac{1-\varphi_{l+1,o}}{1-\varphi_{lo}}\right)^{1/2}\exp\left(-\frac{\xi_l + \xi_{l+1}}{2}\right) + \frac{1}{m} = 0 \quad \text{(III.2)}$$

with λ_l given by

$$\lambda_l = \tfrac{1}{2}(\xi_{l+1} - \xi_l) + \tfrac{1}{2}\log\left(\frac{1-\varphi_{lo}}{1-\varphi_{l+1,o}}\right) \quad \text{(III.3)}$$

It is seen from eq III.1 and III.2 that ξ_l and φ_{lo} are functions of the neighboring variables ξ_{l-1}, ξ_{l+1}, $\varphi_{l-1,o}$, and $\varphi_{l+1,o}$. If values were given for these neighboring variables then eq III.1 and III.2 could be solved for ξ_l and φ_{lo} by Newton's method.

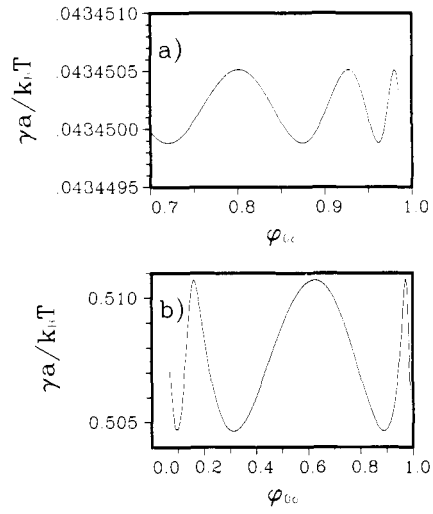

Figure 11. Surface tension as a function of the solvent concentration of the middle lattice layer, φ_{0o}, when the latter variable is artificially fixed. (a) A broad interface characterized by an extremely shallow minimum. (b) A narrow interface with a well-defined minimum.

We have found that, beginning with reasonable sets of $\{\xi_l\}$ and $\{\varphi_{lo}\}$, systematic convergence to a solution can be achieved by the following iterative scheme. Start at level 0 and solve for ξ_o and φ_{0o} holding ξ_1, ξ_{-1}, φ_{1o}, and φ_{-1o} at the initial value. Then, using the new ξ_o and φ_{0o}, and the initial ξ_2 and φ_{2o}, one can solve for ξ_1 and φ_{1o}. Similarly one can go to the level $l = -1$. The process repeats for as many levels as are necessary to essentially approach the asymptotic solutions. The iteration is repeated until some specified convergence criterion is met.

As with most iterative schemes, the initial values must be sensibly chosen if convergent sequences of approximations to $\{\xi_l\}$ and $\{\varphi_{lo}\}$ are to be generated. We have used one of two alternative initializations. In the first case we assume the asymptotic solutions to hold up to the zero level, where a sharp transition occurs. Thus, on the solvent side we start with

$$\varphi_{lo} = 1 \qquad (l < 0) \quad \text{(III.4a)}$$

and from eq III.1

$$\xi_l = \log\varphi_o^* + 2\chi(1 - \varphi_o^*) \qquad (l < 0) \quad \text{(III.4b)}$$

while on the saturated polymer solution side

$$\varphi_{lo} = \varphi_o^* \qquad (l > 0) \quad \text{(III.5a)}$$

$$\xi_l = 0 \qquad (l > 0) \quad \text{(III.5b)}$$

For a broad interface, corresponding to χ not much greater than 0.5, these asymptotic solutions are poor initial approximations in the small $|l|$ region, sometimes leading to divergent sequences of approximants. A better initial set is the final $\{\varphi_{lo}\}$ and $\{\xi_l\}$ determined for a previous χ which is close to the χ of interest. An alternative is to base the initial choice on the Gaussian random-walk model of Helfand and Sapse.[3]

In the case of broad interfaces the convergence of the iterative scheme can be painfully slow. To understand the causes and cure of this affliction let us, for the moment, solve the problem assuming that eq III.1 does not hold for l = 0. In its place we will fix the concentration of solvent, φ_{0o}, on that layer. In Figure 11 we have plotted the surface tension vs. φ_{0o}. The minima are the solutions for which eq III.1

holds for $l = 0$ also. The multiplicity of solutions is due to the arbitrariness as to what is called layer zero; i.e., if for one solution φ_{lo} is the concentration on layer l, there is another solution with the same free energy for which $\varphi_{l-1,o}$ is the concentration on layer l.

For values of φ_{0o} not corresponding to a minimum of the surface tension there is a less than optimal degree of mixing in the layers. The situation is best visualized by considering the more symmetric system of the interface between two immiscible polymers, A and B. The lattice model for this system has been discussed in detail elsewhere,[5] but we will only delve into a quite intuitive aspect of the problem here. There are two solutions to the equations governing this interfacial structure. In the first we have a symmetry about the plane between layers 0 and 1 in the sense that

$$\varphi_{lA} = \varphi_{1-l,B} \qquad \text{(III.6)}$$

where φ_{lK} is the fraction of cells in layer l occupied by units of polymer K. The second solution to the equations has symmetry about the layer $l = 0$, with

$$\varphi_{lA} = \varphi_{-l,B} \qquad \text{(III.7a)}$$

a special case of which is

$$\varphi_{0A} = \varphi_{0B} = \tfrac{1}{2}$$

These two solutions can be embedded in a continuum of possible density profiles resulting from fixing φ_{0A} and relaxing the equation corresponding to eq III.1. In this case we find that the profile corresponding to eq III.6 is a true solution, corresponding to a minimum of the surface tension γ. On the other hand, the solution with $\varphi_{0A} = \frac{1}{2}$ is a surface free energy maximum corresponding to the most mixing in the layers. While the solvent–polymer solution interface is not symmetric like the polymer–polymer interface, still it is clear that certain degrees of mixing are more favorable than others with respect to free-energy minimization.

For the broad interface we see in Figure 11 that the surface tension vs. concentration of solvent in layer zero, φ_{0o}, is quite shallow in its oscillations, only $0.000\,006 k_B T$ per cell. If one is not at an optimal value of φ_{0o} the approach to the solution tends to be quite slow. The way to get around the difficulty is to not leave the adjustments of φ_{0o} to the vagaries of the iterative procedure. Rather, one fixes φ_{0o}, in which case the rest of the solution $\{\varphi_{lo}\}$, $\{\xi_l\}$ rather quickly converges. Then one varies φ_{0o} until the minimum on a curve such as Figure 11 is located.

In mean field theory one accepts only the solution corresponding to the free-energy minimum, but in reality there will be common fluctuations involving states of $0(k_B T)$ away. Therefore, for broad interfaces it can be inferred that the values of concentration found on each layer will be subject to significant fluctuations. This will show up as a further broadening of the interface, for example in x-ray scattering experiments. The values of the surface tension should be less affected. The actual evaluation of free energies to be associated with fluctuations requires that one allow for inhomogeneity in the direction parallel to the interface, which is beyond the scope of this paper, although perhaps not beyond the power of the methods employed.

References and Notes

(1) E. Helfand, *Macromolecules*, preceding paper in this issue, hereafter called paper I.
(2) P. J. Flory, "Principle of Polymer Chemistry", Cornell University Press, Ithaca, N.Y., 1953.
(3) E. Helfand and A. M. Sapse, *J. Polym. Sci.*, to be published.
(4) J. E. Lane, *Aust. J. Chem.*, **21**, 827 (1968).
(5) E. Helfand, *J. Chem. Phys.*, **63**, in press.

Intrachain Reaction of a Pair of Reactive Groups Attached to Polymer Ends. I. Intramolecularly Catalyzed Hydrolysis of a Terminal *p*-Nitrophenyl Ester Group by a Terminal Pyridyl Group on Polysarcosine Chain

Masahiko Sisido,* Takashi Mitamura, Yukio Imanishi, and Toshinobu Higashimura

Department of Polymer Chemistry, Kyoto University, Kyoto 606, Japan. *Received July 17, 1975*

ABSTRACT: The hydrolysis of *p*-nitrophenyl ester groups catalyzed intramolecularly by pyridyl groups, with the two groups attached to two ends of a polysarcosine chain, was investigated. The intrachain reaction rate constant was determined as a function of the degree of polymerization of 5 to 35 at three different temperatures. The rate constant was larger for shorter chains and at higher temperatures. This reaction was compared with the cyclization reaction proceeding on a polymethylene chain taking into account the difference in the inherent reactivity of the end groups. The polysarcosine chain was found to be two or three times more efficient than the polymethylene chain for the intrachain reaction. Activation parameters, $\Delta H_c^{\ddagger}$ and $\Delta S_c^{\ddagger}$, characterizing the conformational change required for the intrachain reaction, were evaluated. $\Delta H_c^{\ddagger}$ as well as $\Delta S_c^{\ddagger}$ increased with increasing chain length. The compensation plot was linear giving an isokinetic temperature of 93 °C. This suggests the possibility to alter the chain length dependence of the intrachain reaction by varying the temperature.

In an X–Y-type polymer the intrachain reactions of a pair of terminal reactive groups, X and Y, will be affected by the conformational properties of the polymer chain in solution. Most polymer chains are sufficiently flexible and if the reaction has a moderately high activation energy, the intrachain collision between X and Y takes place very frequently before the reaction occurs.[1-3] Under these conditions the rate of intrachain reaction is directly proportional to the ring-closure probability, i.e., a probability for a polymer chain to assume conformations in which the end-to-end distance is sufficiently short for the intrachain reaction. The probability will depend upon the chemical structure, chain length, temperature, and other external factors. In other words, it will be possible to control the intrachain reaction by varying these factors.

In 1935, Stoll and Rouvé investigated the esterification